On new solutions for heat transfer in a visco-elastic fluid between parallel plates

ZODWA G MAKUKULA and PRECIOUS SIBANDA
University of KwaZulu-Natal
School of Mathematical Sciences
Private Bag X01, Scottsville, 3209, Pietermaritzburg
SOUTH AFRICA
sibandap@ukzn.ac.za

SANDILE S MOTSA
University of Swaziland
Department of Mathematics
Private Bag 4, Kwaluseni
SWAZILAND
sandilemotsa@gmail.com

Abstract: The steady, laminar flow of a third grade fluid with heat transfer through a flat channel is studied. We propose and apply a successive linearisation method (SLM) and an improved spectral-homotopy analysis method (ISHAM), to obtain approximate analytical solutions for the velocity and temperature profiles. The methods are primarily based on blending non-perturbation techniques with Chebyshev spectral methods to produce efficient algorithms for solving highly nonlinear systems. The effects of the Brinkman number, pressure gradient and the non-Newtonian parameter on the velocity, temperature, skin friction and heat transfer coefficients are discussed. Exact solutions are also constructed and compared with the SLM and ISHAM solutions.

Key–Words: Viscoelastic flow, heat transfer flow, linearisation method, improved spectral-homotopy analysis method, nonlinear BVPs

1 Introduction

The study of non-Newtonian fluids offers many interesting and exciting challenges due to their technical relevance in modelling fluids with complex rheological properties (such as polymer melts, synovial fluids, paints, etc). Viscoelastic fluids also present some highly peculiar characteristics and mathematical features such as the non-unidirectional nature of the flow of such fluids and the increase in the order of the differential equations characterizing such flows, [1, 2]. A lot of work on the flow and heat transfer characteristics of non-Newtonian fluids has also been done in order to control the quality of the end product in many manufacturing and processing industries, see for instance, [1, 3] and the references therein.

Various constitutive models currently exist to describe the properties of non-Newtonian fluids. The major problem however is that none of these models can adequately describe all non-Newtonian fluids. Among the several constitutive equations that have been suggested in the literature is a Rivlin-Erikson model, the third grade fluid model that is capable of describing the normal stress effects for steady unidirectional flow and to predict shear thinning/thickening, [4, 5]. This model has been analyzed in great detail in previous studies by Dunn and Rajagopal [6] and Fosdick and Rajagopal [7].

A large number of recent studies have investigated various aspects of the third-grade fluid model, including some that have merely used this model to test the effectiveness of a slew of new solution techniques for nonlinear equations. Makinde [4] studied the thermal stability of a reactive third-grade liquid flowing steadily between two parallel plates with symmetrical convective cooling at the walls while slip effects on the on the peristaltic flow of a third grade fluid have been studied by among others, Ali et al. [8, 9], El-Shehawy et al. [10] and Motsa et al. [21]. Studies by, among others, Aksoy and Pakdemirli [11], Hayat and his co-workers [12, 13, 14, 15, 16, 17], have, to a large extent, mainly been concerned with the development and testing of new perturbation techniques.

The present study deals with the problem of flow and heat transfer characteristics of a third grade fluid flow between two parallel plates. Exact analytical solutions for the steady Poiseuille flow, the skin friction and the heat transfer coefficients are found. We use innovation, the successive linearisation technique (SLM) (see Makukula et al. [18] and Motsa and Sibanda [20]) and the improved-spectral-homotopy analysis method (ISHAM) to solve the governing nonlinear equations. The accuracy of each methods is determined by comparing the solutions with the exact results.

2 Governing equations

The flow of an incompressible third grade fluid placed between two horizontal parallel impermeable plates is investigated.

The constitutive law for the Cauchy stress tensor $\mathbf{T}$ associated with an incompressible homogeneous fluid of third grade is given in [4, 7, 22]. This has the form

$$\begin{aligned}\mathbf{T} &= -p\mathbf{I}+\mu\mathbf{A}_1+\alpha_1\mathbf{A}_2+\alpha_2\mathbf{A}_1^2+\beta_1\mathbf{A}_3 \\ &\quad +\beta_2[\mathbf{A}_1\mathbf{A}_2+\mathbf{A}_2\mathbf{A}_1]+\beta_3(tr\mathbf{A}_1^2)\mathbf{A}_2, \quad (1)\end{aligned}$$

where

$$\begin{aligned}\mathbf{A}_1 &= \nabla\mathbf{v}+(\nabla\mathbf{v})^T, \\ \mathbf{A}_n &= \frac{d}{dt}(\mathbf{A}_{n-1})+\mathbf{A}_{n-1}\nabla\mathbf{v}+(\nabla\mathbf{v})^T\mathbf{A}_{n-1}.\end{aligned}$$

In the above equations, p is the pressure, μ denotes the viscosity; $\alpha_1, \alpha_2, \beta_1, \beta_2, \beta_3$ are the material moduli, d/dt is the material derivative, $\mathbf{v}$ denotes the velocity field, while $\mathbf{A}_1, \mathbf{A}_2$ and $\mathbf{A}_3$ are the first three Rivlin - Ericksen tensors. The spherical stress $p\,\mathbf{I}$ is due to the constraint of incompressibility. The flow is subject to the restrictions

$$\mu \geq 0,\ \alpha_1 \geq 0,\ |\alpha_1+\alpha_2| \leq \sqrt{24\mu\beta_3} \quad (2)$$

$$\beta_1 = \beta_2 = 0 \quad \text{and} \quad \beta_3 > 0. \quad (3)$$

If $\beta_3 = 0$ the model collapses to that of a second grade fluid. The equations of motion are given by [22, 23];

$$\nabla\cdot\mathbf{v} = 0, \quad (4)$$

$$\rho\frac{d\mathbf{v}}{dt} = \nabla\cdot\mathbf{T}+\rho\mathbf{b}, \quad (5)$$

$$\rho c_p\frac{d\theta}{dt} = \kappa\nabla^2\theta+\mathbf{T}\cdot\nabla\mathbf{v}, \quad (6)$$

where ρ is the mass density, κ the thermal conductivity, c_p is the specific heat at constant pressure, $\mathbf{b}$ is a body force, and θ is the temperature. The x-axis tangential to the plate surface, the y-axis normal to it. The fluid is confined between parallel plates located at $y = -h$ and $y = h$. We assume unidirectional flow so that

$$\mathbf{v} = u(y)\mathbf{i} \quad \text{and} \quad \theta = \theta(y).$$

The temperature of the upper plate is maintained at θ_1 and that of lower plate at θ_0 to give a temperature difference $\Delta\theta = \theta_1 - \theta_0$. The fluid motion is driven either by a constant pressure gradient or by the boundary conditions. Equations (4) - (6) reduce to (see, [4, 22, 21]);

$$\frac{d^2u}{dy^2}\left[1+6\beta\left(\frac{du}{dy}\right)^2\right] = -B, \quad (7)$$

$$\frac{d^2\theta}{dy^2}+\lambda\left(\frac{du}{dy}\right)^2\left[1+2\beta\left(\frac{du}{dy}\right)^2\right] = 0, \quad (8)$$

where

$$\begin{aligned}\beta &= \frac{\beta^* U^2}{\mu\, h^2},\ \lambda = \frac{\mu U^2}{\kappa\Delta\theta}, \\ B &= -\frac{h^2}{\mu U}\frac{dp}{dx}, \quad \beta^* = \beta_2+\beta_3.\end{aligned}$$

The parameters are the characteristic velocity U and the Brinkman number λ which determines the relative importance between the viscous dissipation and fluid conduction.

The appropriate boundary conditions are

$$u(-1) = 0, \quad u(1) = 0 \quad (9)$$

$$\theta(-1) = 0, \quad \theta(1) = 1. \quad (10)$$

In a recent study Motsa et al. [21] showed that the exact solution for the skin friction is

$$u'(y) = \frac{1}{6\beta}[F(y)]^{1/3}-[F(y)]^{-1/3}, \quad (11)$$

where

$$F(y) = 6\beta^2\left[-9By+\sqrt{\frac{6+81\beta By^2}{\beta}}\right]. \quad (12)$$

It is evident that this result is only valid when

$$\beta \geq -\frac{2}{27B^2}.$$

The temperature equation now simplifies to

$$\theta'' = \lambda By\, u'(y). \quad (13)$$

Equation (13) can easily be solved using any numerical method.

3 The linearisation method

In this section we apply the successive linearisation method (SLM) to solve equations (7) - (10). Since equation (7) is decoupled from the temperature equation (8) we only need apply the SLM to equation (7). The SLM is based on the assumptions that

- the unknown function $u(y)$ can be expanded as

$$u(y) = U_i(y)+\sum_{n=0}^{i-1}u_n(y),\ i = 1, 2, 3, \ldots \quad (14)$$

where U_i are unknown functions and u_n are approximations which are obtained by recursively solving the linear part of the equation that results from substituting (14) in equation (7), and that

- U_i becomes increasingly smaller as i becomes large, that is

$$\lim_{i\to\infty} U_i = 0. \tag{15}$$

Substituting (14) in equation (7) and neglecting nonlinear terms in U_i, U_i', U_i'' and using $U_i \approx u_i$ gives

$$\begin{aligned}&\left[1+6\beta\left(\sum_{n=0}^{i-1}u_n'\right)^2\right]u_i''\\&+\left[12\beta\sum_{n=0}^{i-1}u_n'\sum_{n=0}^{i-1}u_n''\right]u_i' = -B+\sum_{n=0}^{i-1}u_n''\\&+6\beta\left(\sum_{n=0}^{i-1}u_n'\right)^2\sum_{n=0}^{i-1}u_n'',\end{aligned} \tag{16}$$

which may be written in a more compact form as,

$$a_{i-1}u_i'' + b_{i-1}u_i' = r_{i-1}, \tag{17}$$

subject to the boundary conditions

$$u_i(-1) = u_i(1) = 0, \tag{18}$$

where,

$$\begin{aligned}a_{i-1} &= 1+6\beta\left(\sum_{n=0}^{i-1}u_n'\right)^2,\\ b_{i-1} &= 12\beta\sum_{n=0}^{i-1}u_n'\sum_{n=0}^{i-1}u_n'',\\ r_{i-1} &= -\left[B+\sum_{n=0}^{i-1}u_n''+6\beta\left(\sum_{n=0}^{i-1}u_n'\right)^2\sum_{n=0}^{i-1}u_n''\right].\end{aligned}$$

Once each solution u_i $(i \geq 1)$ has been found by iteratively solving equations (16), starting from an initial approximation $u_0(y)$, the approximate solutions for $u(y)$ are obtained as

$$u(y) \approx \sum_{n=0}^{M} u_n(y) \tag{19}$$

where M is the order of the SLM approximation. The initial approximation $u_0(y)$ is chosen in such a way that it satisfies the boundary conditions (9). In this study, a suitable initial approximation was chosen to be

$$u_0(y) = 0. \tag{20}$$

We observe that, by making use of the symmetry condition $u_i'(0) = 0$, equation (16) has an integrating factor (IF) given by

$$IF = 1+6\beta\left(\sum_{n=0}^{i-1}u_n'\right)^2. \tag{21}$$

Integrating (16) gives

$$u_i' = -\frac{1}{IF^2}\left[By+\sum_{n=0}^{i-1}u_n'+2\beta\left(\sum_{n=0}^{i-1}u_n'\right)^3\right]. \tag{22}$$

Thus starting from an initial guess $u_0(y) = 0$, the solutions for u_i $(i \geq 1)$ can be obtained iteratively from equation (16). The first three solutions for $i = 1, 2, 3, ...,$ are given as

$$u_1'(y) = -By, \tag{23}$$

$$u_2'(y) = \frac{2\beta B^3 y^3}{1+6\beta B^2 y^2}, \tag{24}$$

$$u_3'(y) = -\frac{-8\beta^3 B^7 y^7(3+16\beta B^2 y^2)}{k_1(1+6k_2\beta B^2 y^2)}, \tag{25}$$

where

$$\begin{aligned}k_1 &= 1+6\beta B^2 y^2,\\ k_2 &= 3+14\beta B^2 y^2+16\beta^2 B^4 y^4.\end{aligned}$$

The explicit solutions for $u_4', u_5', u_6', \ldots$ can be obtained in the same manner.

The analytic solution for the skin friction coefficient C_f is obtained as

$$u'(1) \approx u_0'(1)+u_1'(1)+u_2'(1)+u_3'(1)+\ldots \tag{26}$$

Since the coefficient parameters and the right hand side of equation (16), for $i = 1, 2, 3, \ldots$, are known (from previous iterations), equation (16) can easily be solved using analytical means or numerical methods. Solving equation (16) analytically for u_i was only possible for the first two iterations. For higher order iterations $(i > 3)$ numerical integration was employed. In this work, equations (16) was integrated using the Chebyshev spectral collocation method. This method is based on approximating the unknown functions by the Chebyshev interpolating polynomials in such a way that they are collocated at the Gauss-Lobatto points defined as

$$y_j = \cos\frac{\pi j}{N}, \quad j = 0, 1, \ldots, N. \tag{27}$$

where N is the number of collocation points used. The second derivative of u_i at the collocation points are represented as

$$\frac{d^2u_i}{dy^2} = \sum_{k=0}^{N}\mathbf{D}_{kj}^2 u_i(y_k), \quad j = 0, 1, \ldots, N \tag{28}$$

where $\mathbf{D}$ is the Chebyshev spectral differentiation matrix. Substituting equations (27) - (28) in (17) results in the matrix equation

$$\mathbf{A}_{i-1}\mathbf{U}_i = \mathbf{R}_{i-1}, \tag{29}$$

with boundary conditions

$$u_i(y_0) = u_i(y_N) = 0, \tag{30}$$

in which $\mathbf{A}_{i-1}$ is a $(N+1)\times(N+1)$ square matrix and $\mathbf{U}_i$ and $\mathbf{R}_{i-1}$ are $(N+1)\times 1$ column vectors defined by

$$\begin{aligned}\mathbf{U}_i &= [u_i(y_0),\ldots,u_i(y_{N-1}),u_i(y_N)]^T,\\ \mathbf{R}_{i-1} &= [r_{i-1}(y_0),\ldots,r_{i-1}(y_{N-1}),r_{i-1}(y_N)]^T,\\ \mathbf{A}_{i-1} &= \mathbf{a}_{i-1}\mathbf{D}^2+\mathbf{b}_{i-1}\mathbf{D},\end{aligned}$$

where $\mathbf{b}_{i-1}$ is a diagonal matrix of size $(N+1)\times(N+1)$. After modifying the matrix system (29) to incorporate boundary conditions (30), the solution is obtained as

$$\mathbf{U}_i = \mathbf{A}_{i-1}^{-1}\mathbf{\Phi}_{i-1}. \tag{31}$$

The solution for $\theta(y)$ is obtained by applying the Chebyshev spectral collocation method to (13).

4 The improved spectral homotopy analysis method (ISHAM)

In this section we describe and apply the ISHAM to solve the governing equation (7) with boundary conditions (10). The ISHAM algorithm seeks to improve the initial approximation that is then used in the original SHAM [19] algorithm to solve the governing nonlinear equation. The basic assumption is that the solution $u(y)$ can be expanded as

$$u(y) = U_i(y) + \sum_{n=0}^{i-1} u_n(y), \quad i = 1,2,3,\ldots, \tag{32}$$

where U_i are unknown functions whose solutions are obtained using the SHAM algorithm at the ith iteration and $u_n(y)$, $(n \geq 1)$ are known from previous iterations. The algorithm begins with an initial approximation

$$u_0(y) = \alpha B(1-y^2), \tag{33}$$

which is chosen to satisfy the boundary conditions (10) and α is a scaling parameter. Substituting equation (32) and using $U_i \approx u_i$ in the governing equation (7) gives

$$a_{1,i-1}u_i'' + a_{2,i-1}u_i' + 6\beta u_i''(u_i')^2 = r_{i-1}, \tag{34}$$

subject to the boundary conditions

$$u_i(-1) = u_i(1) = 0, \tag{35}$$

where the coefficient parameters $a_{k,i-1}$ $(k = 1,2)$, r_{i-1} are defined as

$$\begin{aligned}a_{1,i-1} &= 1+6\beta\left(\sum_{n=0}^{i-1}u_n'\right)^2,\\ a_{2,i-1} &= 12\beta\sum_{n=0}^{i-1}u_n'\sum_{n=0}^{i-1}u_n'',\\ r_{i-1} &= -\left[B+\sum_{n=0}^{i-1}u_n''+6\beta\left(\sum_{n=0}^{i-1}u_n'\right)^2\sum_{n=0}^{i-1}u_n''\right].\end{aligned}$$

Starting from the initial approximation (33) the subsequent solutions u_i, $(i \geq 1)$ are obtained by recursively solving equation (34) using the SHAM approach. To find the SHAM solutions of (34) we begin by defining the following linear operator

$$\mathcal{L}[\mathcal{U}_i(y;q)] = a_{1,i-1}\frac{\partial^2\mathcal{U}_i}{\partial y^2} + a_{2,i-1}\frac{\partial\mathcal{U}_i}{\partial y}, \tag{36}$$

where $q \in [0,1]$ is the embedding parameter, and $\mathcal{U}_i(y;q)$ are unknown functions. The zeroth order deformation equation is given by

$$(1-q)\mathcal{L}[\mathcal{U}_i(y;q) - u_{i,0}(y)] = q\hbar\mathcal{N}[\mathcal{U}_i(y;q)] - r_{i-1}, \tag{37}$$

where $\hbar$ is the non-zero convergence controlling auxiliary parameter and $\mathcal{N}$ is a nonlinear operator given by

$$\mathcal{N}[\mathcal{U}_i(y;q)] = a_{1,i-1}\frac{\partial^2\mathcal{U}_i}{\partial y^2} + a_{2,i-1}\frac{\partial\mathcal{U}_i}{\partial y} + 6\beta\frac{\partial^2\mathcal{U}_i}{\partial y^2}\left(\frac{\partial\mathcal{U}_i}{\partial y}\right)^2. \tag{38}$$

Differentiating (37) m times with respect to q and then setting $q = 0$ and finally dividing the resulting equations by $m!$ yields the mth order deformation equations

$$\begin{aligned}&\mathcal{L}[u_{i,m}(y) - \chi_m u_{i,m-1}(y)] = \\ &\hbar\left(a_{1,i-1}u_{i,m-1}'' + a_{2,i-1}u_{i,m-1}'\right.\\ &\left.+6\beta\sum_{j=0}^{m-1}u_{i,m-1-j}''\sum_{n=0}^{j}u_{i,j-n}'u_{i,n}' - (1-\chi_m)r_{i-1}\right),\end{aligned} \tag{39}$$

subject to the boundary conditions

$$u_{i,m}(-1) = u_{i,m}(1) = 0, \tag{40}$$

where

$$\chi_m = \begin{cases}0, & m \leq 1\\ 1, & m > 1\end{cases}. \tag{41}$$

The initial approximation $u_{i,0}$ that is used in the higher order equation (39) is obtained by solving the linear part of equation (34) given by

$$a_{1,i-1}u''_{i,0} + a_{2,i-1}u'_{i,0} = r_{i-1}, \tag{42}$$

with the boundary conditions

$$u_{i,0}(-1) = u_{i,0}(1) = 0. \tag{43}$$

Applying the Chebyshev spectral method, described in the SLM section, to solve equation (42) yields the matrix form

$$\mathbf{A}_{i-1}\mathbf{U}_{i,0} = \mathbf{Q}_{i-1}, \tag{44}$$

subject to the boundary conditions

$$u_{i,0}(y_0) = \quad u_{i,0}(y_N) = 0, \tag{45}$$

where

$$\begin{aligned} \mathbf{A}_{i-1} &= \mathbf{a}_{1,i-1}\mathbf{D}^2 + \mathbf{a}_{2,i-1}\mathbf{D}, \\ \mathbf{U}_{i,0} &= [u_{i,0}(y_0), u_{i,0}(y_1), \ldots, u_{i,0}(y_N)]^T, \\ \mathbf{Q}_{i-1} &= [r_{i-1}(y_0), r_{i-1}(y_1), \ldots, r_{i-1}(y_N)]^T. \end{aligned} \tag{46}$$

After modifying the matrix system (44) to incorporate the boundary conditions (45), the solution is obtained as

$$\mathbf{U}_{i,0} = \mathbf{A}_{i-1}^{-1}\mathbf{Q}_{i-1}. \tag{47}$$

Similarly, applying the Chebyshev spectral transformation on the higher order deformation equation (39) gives

$$\begin{aligned} \mathbf{A}_{i-1}\mathbf{U}_{i,m} &= (\chi_m + \hbar)\mathbf{A}_{i-1}\mathbf{U}_{i,m-1} \\ &- \hbar(1-\chi_m)\mathbf{Q}_{i-1} + \hbar\mathbf{P}_{i,m-1}, \end{aligned} \tag{48}$$

where $\mathbf{A}_{i-1}$ and $\mathbf{Q}_{i-1}$, are as defined in (46) and

$$\begin{aligned} \mathbf{U}_{i,m} &= [u_{i,m}(y_0), u_{i,m}(y_1), \ldots, u_{i,m}(y_N)]^T, \\ \mathbf{P}_{i,m-1} &= 6\beta \sum_{j=0}^{m-1} \mathbf{D}^2 u_{i,m-1-j} \sum_{n=0}^{j} \mathbf{D}u_{i,j-n}\mathbf{D}u_{i,n}. \end{aligned}$$

To implement the boundary conditions on the right hand side of equation (48), we set the first and last rows and columns of $\mathbf{A}_{i-1}$ to be zero and similarly the first and last columns of $\mathbf{Q}_{i-1}$ and $\mathbf{P}_{m-1}$ to be zero. This results in the following recursive formula for $m \geq 1$

$$\begin{aligned} \mathbf{U}_{i,m} &= (\chi_m + \hbar)\mathbf{A}_{i-1}^{-1}\tilde{\mathbf{A}}_{i-1}\mathbf{U}_{i,m-1} \\ &+ \hbar\mathbf{A}_{i-1}^{-1}[\mathbf{P}_{i,m-1} - (1-\chi_m)\mathbf{Q}_{i-1}], \end{aligned} \tag{49}$$

where $\tilde{\mathbf{A}}_{i-1}$ is the modified matrix $\mathbf{A}_{i-1}$ on the right hand side of (48) after incorporating the boundary conditions. Thus starting from the initial approximation, which is obtained from (47), higher order approximations $u_{i,m}(y)$ for $m \geq 1$, can be obtained through the recursive formula (49). The solutions for u_i are then generated using the solutions for $u_{i,m}$ as follows

$$u_i = u_{i,0} + u_{i,1} + u_{i,2} + u_{i,3} + \ldots + u_{i,m}. \tag{50}$$

The $[i, m]$ approximate solution for $u(y)$ is then obtained by substituting u_i obtained from (50) into equation (32).

5 Results and Discussion

In this section we present a comparison of the successive linearisation method (SLM), improved spectral-homotopy analysis method (ISHAM) and the exact analytical results. All the SLM and ISHAM results were generated using $N = 100$ collocation points. To show the accuracy and effectiveness of the methods, a limited parametric study is undertaken.

Table 1 shows a comparison of the convergence rate of the SLM, ISHAM and the exact solution when $B = 1$ and for increasing values of the non-Newtonian parameter β. A match between the SLM results and the exact results, accurate to 10 decimal places is achieved at the sixth order of the SLM series solution for all the selected values of β while the ISHAM converges to the exact solution at order [4,4]. The difference in convergence rates of the two methods is clearly shown in Table 2 where a comparison of the absolute errors in the SLM and ISHAM approximate solutions for $u'(1)$ is given for various values of β when $B = 1$.

In Table 3 the non-Newtonian parameter is fixed at $\beta = 1$ while the pressure gradient term increases monotonically from $\beta = 0.2$. For $B \leq 1$, full convergence of the SLM approximations to the exact solution is achieved at the fourth-order of the SLM series solution while the ISHAM converges at order [3,3]. The precision of the SLM however deteriorates faster than that of the ISHAM with increasing B with more terms needed in the SLM series to match the exact results. Full convergence to the exact results (to ten decimal places) is achieved at the 4th order of the SLM series for $B \leq 1$ and at order [3,3] for ISHAM solutions. For $B > 1$ The SLM converges fully at the sixth order of approximation while the ISHAM approximate solutions converge at order [4,4]. These is clearly indicated in Table 4 where a comparison of the absolute errors between the SLM and ISHAM approximate solutions for $u'(1)$ are given for various values of B when $\beta = 1$.

Table 1: Comparison of the approximate values of $u(1)$ using the SLM and ISHAM with the exact solution for various values of β when $B = 1$.

SLM solution					
β	3rd order	4th order	5th order	6th order	Exact
0.2	-0.7972810885	-0.7972810583	-0.7972810583	-0.7972810583	-0.7972810583
0.5	-0.6823395826	-0.6823278039	-0.6823278038	-0.6823278038	-0.6823278038
1.0	-0.5900220423	-0.5897545943	-0.5897545123	-0.5897545123	-0.5897545123
2.0	-0.5023901750	-0.5000085354	-0.5000000001	-0.5000000000	-0.5000000000
ISHAM solution					
	[2,2]	[3,3]	[4,4]	[5,5]	Exact
0.2	-0.7972810449	-0.7972810583	-0.7972810583	-0.7972810583	-0.7972810583
0.5	-0.6823218302	-0.6823278038	-0.6823278038	-0.6823278038	-0.6823278038
1.0	-0.5896283020	-0.5897545122	-0.5897545123	-0.5897545123	-0.5897545123
2.0	-0.4991584068	-0.4999999475	-0.5000000000	-0.5000000000	-0.5000000000

Table 2: Comparison of the absolute errors between the SLM and ISHAM approximate solutions for $u(1)$ and the exact solution for various values of β when $B = 1$.

SLM solution				
β	3rd order	4th order	5th order	6th order
0.2	0.0000000302	0.0000000000	0.0000000000	0.0000000000
0.5	0.0000117788	0.0000000001	0.0000000000	0.0000000000
1.0	0.0002675300	0.0000000820	0.0000000000	0.0000000000
2.0	0.0023901750	0.0000085354	0.0000000001	0.0000000000
ISHAM solution				
	[2,2]	[3,3]	[4,4]	[5,5]
0.2	0.0000000134	0.0000000000	0.0000000000	0.0000000000
0.5	0.0000059736	0.0000000000	0.0000000000	0.0000000000
1.0	0.0001262103	0.0000000001	0.0000000000	0.0000000000
2.0	0.0008415932	0.0000000525	0.0000000000	0.0000000000

Table 3: Comparison of the approximate values of $u(1)$ using the SLM and ISHAM with the exact solution for various values of B when $\beta = 1$.

SLM solution					
B	3rd order	4th order	5th order	6th order	Exact
0.2	-0.1869351878	-0.1869351878	-0.1869351878	-0.1869351878	-0.1869351878
0.5	-0.3854585785	-0.3854584985	-0.3854584985	-0.3854584985	-0.3854584985
1.0	-0.5900220423	-0.5897545943	-0.5897545123	-0.5897545123	-0.5897545123
2.0	-0.8564235361	-0.8355504792	-0.8351225255	-0.8351223485	-0.8351223485
ISHAM solution					
	[2,2]	[3,3]	[4,4]	[5,5]	Exact
0.2	-0.1869351878	-0.1869351878	-0.1869351878	-0.1869351878	-0.1869351878
0.5	-0.3854584608	-0.3854584985	-0.3854584985	-0.3854584985	-0.3854584985
1.0	-0.5896283020	-0.5897545122	-0.5897545123	-0.5897545123	-0.5897545123
2.0	-0.8318383437	-0.8351152280	-0.8351223485	-0.8351223485	-0.8351223485

Table 4: Comparison of the absolute errors between the SLM and ISHAM approximate solutions for $u(1)$ and the exact solution for various values of B when $\beta = 1$.

SLM solution				
B	3rd order	4th order	5th order	6th order
0.2	0.0000000000	0.0000000000	0.0000000000	0.0000000000
0.5	0.0000000800	0.0000000000	0.0000000000	0.0000000000
1.0	0.0002675300	0.0000000820	0.0000000000	0.0000000000
2.0	0.0213011876	0.0004281307	0.0000001770	0.0000000000
ISHAM solution				
	[2,2]	[3,3]	[4,4]	[5,5]
0.2	0.0000000000	0.0000000000	0.0000000000	0.0000000000
0.5	0.0000000377	0.0000000000	0.0000000000	0.0000000000
1.0	0.0001262103	0.0000000001	0.0000000000	0.0000000000
2.0	0.0032840048	0.0000071205	0.0000000000	0.0000000000

Figure 1 shows the velocity distribution for the Poiseuille flow with β as calculated using the successive linearisation method. The velocity profiles decrease with β. These results are accurate and qualitatively similar to those obtained by Roohi et al. [25] using the HAM, Motsa et al. [21] using the spectral homotopy analysis method and Siddique et al. [22] using the homotopy perturbation method.

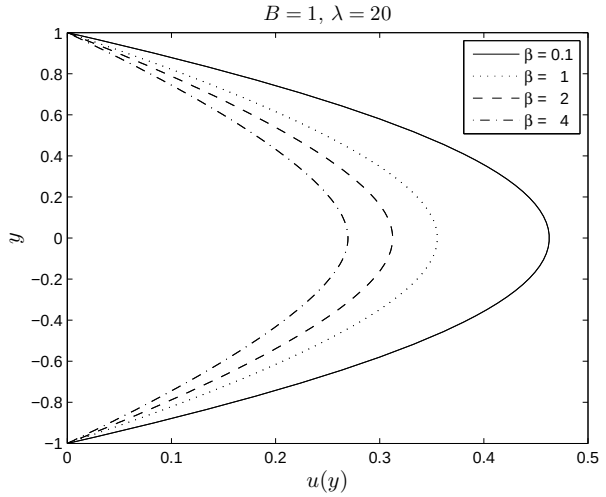

Figure 1: Velocity $u(y)$ profiles for different values of β

Figure 2 shows the effect of the pressure gradient on the temperature profiles for fixed $\beta = 1$ and $\lambda = 20$. Figure 3 shows the effect of the Brinkman number which determines the relative importance between viscous dissipation effects and fluid conduction on the temperature profiles for fixed B and β. Simulations show that as the Brinkman number increases, more heat is generated by the viscous dissipation effect and the temperature rapidly increases with λ, (see also Saouli et al. [26]).

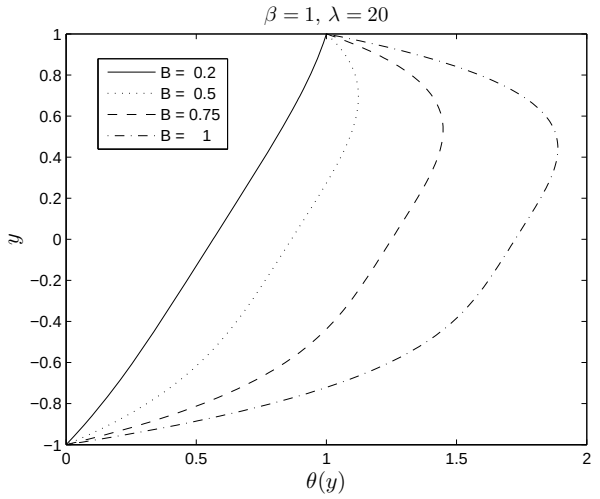

Figure 2: Temperature $\theta(y)$ profiles for different values of B

Figure 4 shows the variation of the skin-friction with B and β for fixed λ. The skin friction increases with β for increasing pressure gradient.

Figure 5 shows the growth of the wall heat transfer rate for various values of the parameter B. Increasing B increases the heat transfer rate.

6 Conclusion

In the present paper we considered the steady laminar flow of a third grade fluid with heat transfer through a flat channel. Two algorithms, namely the successive linearisation method (SLM) and the improved spectral-homotopy analysis method (ISHAM) were

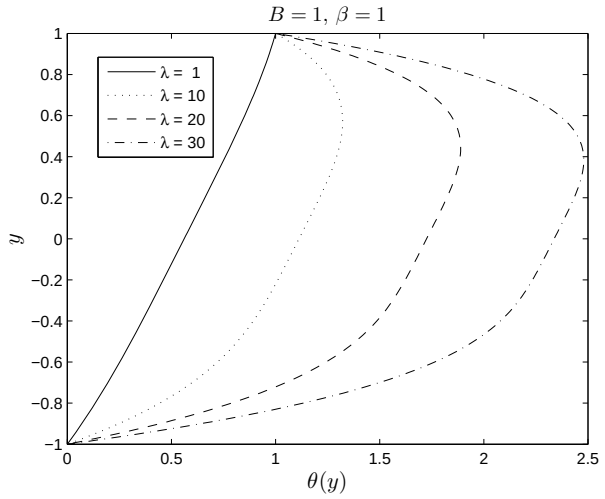

Figure 3: Temperature $\theta(y)$ profiles for different values of λ

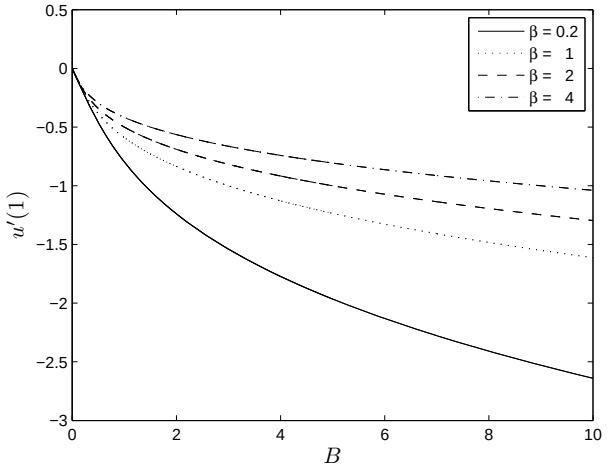

Figure 4: Skin friction $u'(1)$ for different values of B

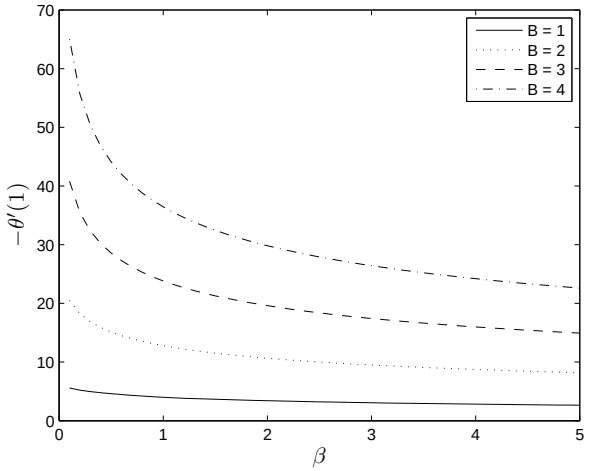

Figure 5: Wall heat transfer rate $-\theta'(1)$ for different values of β when $\lambda = 20$

presented to compute the analytical results for the skin friction coefficient and rate of heat transfer. New analytical results for the skin friction at the channel walls have been found. A comparison of the rate of convergence of the SLM and ISHAM approximations to the exact result shows that while both methods converge rapidly, the ISHAM however converges much more rapidly than the SLM. Both methods converge for all parameter values with the ISHAM showing better convergence for larger parameter values. The SLM and ISHAM were both applied successfully to compute the analytical results for the steady laminar flow of a third grade fluid with heat transfer through a flat channel. The success together with consistency of our results with earlier findings shows that the two methods can be efficiently used to solve nonlinear problems in science and engineering.

References

[1] P. D. Ariel, Flow of a third grade fluid through a porous flat channel, *International Journal of Engineering Science*, Vol. 41, 2003, pp. 1267 – 1285.

[2] K. Fakhar, Exact solutions for nonlinear partial differential equation arising in third grade fluid flows, *Southeast Asian Bulletin of Mathematics*, Vol. 32, 2008, pp. 65 – 70.

[3] T. Altan, H. Gegel, *Metal forming fundamentals and applications*, American Society of Metals, Metals Park, OH, 1979.

[4] O. D. Makinde, On thermal stability of a reactive third-grade fluid in a channel with convective cooling the walls, *Appl. Math. Comp*., Vol. 213, 2009, pp. 170 – 176.

[5] M. Yurusoy, M. Pakdemirli, Approximate analytical solutions for the flow of a third grade fluid in a pipe, *Int. J. Non-Linear Mech.*, Vol. 37, 2002, pp. 187-195.

[6] J. E. Dunn and K. R. Rajagopal, Fluids of differential type: critical review and thermodynamic analysis, *Int. J. Engrg. Sci*., Vol. 33 no. 5, 1995, pp. 689-729.

[7] R. L. Fosdick, K. R. Rajagopal, Thermodynamics and stability of fluids of third grade, *Proc. Roy. Soc. London A*, Vol. 369, 1980, pp. 351 – 377.

[8] N. Ali, Y. Wang, T. Hayat, M. Oberlack, Slip Effects on the Peristaltic Flow of a Third Grade Fluid in a Circular Cylindrical Tube *J. Appl. Mech*., Vol.76, 2009, 011006 (10 pages) doi:10.1115/1.2998761

[9] N. Ali, T. Hayat, Y. Wang, MHD peristaltic flow of a third order fluid in an asymmetric channel, *International Journal for Numerical Methods in Fluids*, 2009 DOI: 10.1002/fld.2184.

[10] E. F. El-Shehawy, N. T. El-Dabe, I. M. El-Desoky, Slip Effects on the Peristaltic Flow of a Non-Newtonian Maxwellian Fluid, *Acta Mech*., Vol. 186, 2006, pp. 141-159.

[11] Y. Aksoy, M. Pakdemirli, Approximate Analytical Solutions for Flow of a Third-Grade Fluid Through a Parallel-Plate Channel Filled with a Porous Medium, *Journal Transport in Porous Media*, 2009; doi:10.1007/s11242-009-9447-5

[12] T. Hayat, N. Ahmed, M. Sajid, Analytic solution for MHD flow of a third order fluid in a porous channel, *J. Comp. Appl. Math*., Vol. 214, 2008, pp. 572–582.

[13] T. Hayat, R. Ellahi, F.M. Mahomed, Exact solutions for thin film flow of a third grade fluid down an inclined plane, *Chaos Solit. Fract*., Vol. 38(5), 2008, pp. 1336–1341.

[14] T. Hayat, M. Khan, M. Ayub, On the explicit analytic solutions of an Oldroyd 6-constant fluid, *Int. J. Eng. Sci*., Vol. 42, 2004, pp. 123–135.

[15] T. Hayat, S. Asghar, and A. M. Siddiqui, Periodic unsteady flows of a non-Newtonian fluid, *Acta Mech. Vol*., 131 no. 3-4, 1998, pp. 169-175.

[16] T. Hayat, R. Naz, M. Sajid, On the homotopy solution for Poiseulle flow of a fourth grade fluid, *Commun. Nonlinear Sci. Numer. Simul*., 2009, doi:10.1016/j.cnsns.2009.04.024.

[17] T. Hayat, R. Ellahi, P.D. Ariel, and S. Asghar, Homotopy solutions for the channel flow of a third grade fluid, *Nonlin. Dyn*. Vol. 45, 2006, pp. 55–64.

[18] Z. Makukula, S. S. Motsa and P. Sibanda, "On a new solution for the viscoelastic squeezing flow between two parallel plates, *Journal of Advanced Research in Applied Mathematics*, vol. 2, no. 4, 2010, pp. 31 - 38.

[19] S.S. Motsa, P. Sibanda, S. Shateyi, A new spectral-homotopy analysis method for solving a nonlinear second order BVP, Commun. Nonlinear Sci. Numer. Simul., 15 (2010) 2293 – 2302.

[20] S. S. Motsa and P. Sibanda, *A new algorithm for solving singular IVPs of Lane-Emden type*, Proceedings of the 4th International Conference on Applied Mathematics, Simulation, Modelling, pp. 176 - 180, NAUN International Conferences, Corfu Island, Greece, July 22-25, 2010.

[21] S. S. Motsa, Z. G. Makukula and P. Sibanda, A spectral-homotopy analysis method for heat transfer flow of a third grade fluid between parallel plates, *International Journal of Numerical Methods for Heat and Fluid Flow*, 2010, in press.

[22] A.M. Siddiqui, A.Zeb, Q.K. Ghori, A.M. Benharbit, Homotopy perturbation method for heat transfer flow of a third grade fluid between parallel plates, *Chaos Solit. Frac.*, Vol. 36, 2008, pp. 182–192.

[23] S. Asghar, M. R. Mohyuddin, T. Hayat, A. M. Siddiqui, The flow of a non-Newtonian fluid induced Due to the oscillations of a porous plate, *Mathematical Problems in Engineering* Vol. 2004: 2, 2004, pp. 133143, URL: http://dx.doi.org/10.1155/S1024123X04309014.

[24] S.J. Liao, Beyond perturbation: *Introduction to homotopy analysis method.* Chapman & Hall/CRC Press, 2003.

[25] E. Roohi, S. Kharazmi, Y. Farjami, Application of the homotopy method for analytical solution of non-Newtonian channel flows, *Phys. Scr.*, 2009, doi:10.1088/0031-8949/79/06/065009.

[26] S. Saouli, S. Aiboud-Saouli, Second-law analysis of laminar nonnewtonian gravity-driven liquid film along an inclined heated plate with viscous dissipation effect, *Braz. J. Chem. Eng.*, Vol. 26, 2009, doi: 10.1590/S0104-66322009000200019.